IEEE Access
Multidisciplinary | Rapid Review | Open Access Journal

SPECIAL SECTION ON ADVANCED MODELING AND CONTROL OF COMPLEX MECHATRONIC SYSTEMS WITH NONLINEARITY AND UNCERTAINTY

Received August 4, 2018, accepted September 4, 2018, date of publication September 10, 2018, date of current version October 8, 2018.

Digital Object Identifier 10.1109/ACCESS.2018.2869386

Nonlinear Dynamics Modeling and Analysis of Underwater Mud-Penetrator Steering System

YINGLONG CHEN[1], (Member, IEEE), HUI LIU[1,2], ZENGMENG ZHANG[1], JIAOYI HOU[1], AND YONGJUN GONG[1]

[1]Naval Architecture and Ocean Engineering College, Dalian Maritime University, Dalian 116026, China
[2]School of Naval Architecture, Dalian University of Technology, Dalian 116024, China

Corresponding author: Zengmeng Zhang (zzm.zju@163.com)

This work was supported in part by the Fundamental Research Funds for the Central Universities under Grant 017183018 and in part by the Doctoral Scientific Research Foundation of Liaoning Province under Grant 201501137.

ABSTRACT Adopting underwater mud-penetrator to thread the steel wire is one of the important steps in the current wreck salvage process, which is safer and more efficient than threading with manpower by the diver. This paper first establishes the kinematics model of the underwater mud-penetrator in the inertial coordinate system and discussed the drill steering mechanism and force characteristics under the nonlinear coupling interaction between drill bit, drill pipe, and seabed geology. Based on the Newton–Eulerian method, the nonlinear dynamic model of mud-penetrator is established, and the influence of guiding angle, geological features, and propelling force on steering process is analyzed through simulation. The simulation results show that the steering process of underwater mud-penetrator is the compound movement of the drill bit translation and deflection. The reduction of the guiding angle and the increase of the propulsive force can effectively improve the guiding ability of the non-excavation drill bit. As the guiding angle decreases pi/12–pi/15, the deflection angle of the drill bit is increased by 2°–3°, and as propulsion increases 500 N, the deflection angle of the drill bit is increased by 3°. The area of the guiding plate also has a great influence on the guiding ability of the drill bit, and the deflection angle is inversely proportional to the area of the drill guiding plate. The deflection angle is more sensitive to soft geological changes. The simulation results are of great significance help to understand the process of drilling guidance process for wrecking and salvaging, and it can help to improve the threading success rate and salvage efficiency.

INDEX TERMS Underwater mud-penetrator, threading steel wire, steering system, nonlinear dynamics.

I. INTRODUCTION

With the increasing global marine economic activities, the number of sea wrecks is rising, and the difficulty of salvaging the wreck is gradually increasing [1], [2]. Threading steel wire is a key link in the process of wreck salvage [3]–[5], which is used to supply supporting force of steel wire to lift the wreck as shown in Fig. 1. However, among the several salvaging steps threading steel wire is most time-consuming, which often accounts for more than half of the salvage period [6]. The success of salvaging shipwreck operations is closely related to the efficiency, quality and precision of threading wire [1], [6].

However, in some wrecking salvage project, the task of threading the steel wire is still completed by the diver underwater with manpower, and the work efficiency is low, the work accuracy is poor, the safety of the diver cannot be guaranteed. Underwater mud-penetrator is development of non-excavation technology which is designed for the underwater engineering especially for the threading steel wire of salvage project. With the development of non-excavation technology, underwater mud-penetrator can be used to complete the threading task [7], [8] instead of diver, which can

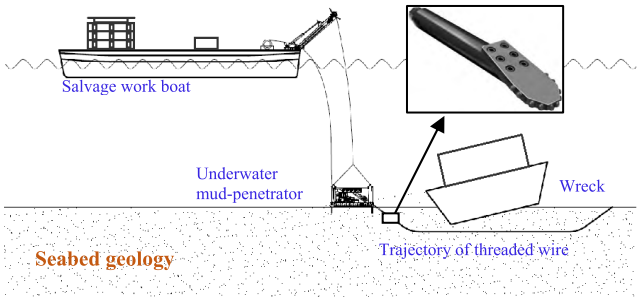

FIGURE 1. Underwater mud-penetrator threading wire.

improve the efficiency of the threading, shorten the construction period, and increase the success rate of salvage shipwreck salvage so as to better cope with the unexpected events such as sinking at sea.

However, the underwater movement of the drill bit of mud-penetrator is very complicated, and steering process is a strongly nonlinear system with the features of complex structure and strong coupling with mud and drill pipe. In order to complete the threading task under different seabed geological conditions, it is necessary to accurately predict and the motion of the drill bit [9], give full play to the drilling guidance ability, and achieve precise control of the optimal threading trajectory. First importantly, an accurate and nonlinear drill guiding dynamics model needs to be established to achieve these requirements [10], [11].

The numerical simulation is used to study and verify the drilling mechanism of the drill bit under static and dynamic loads, and fully understand the real-time interaction between the drill bit and the rock [12], [13], so as to clarify the change of soil resistance [14] and resistance torque [15] when the drill bit is drilled. However, the drilling guidance mechanism and the force of the drill bit are directly related to its structure, due to the different structure of the non-excavated drill bit, the soil resistance and guiding mechanism still need further research. Thereby accurately calculating the variation law of the resistance during the drilling process.

The establishment of the PDC drill bit dynamics model is more reflected in the study of the dynamic model of drilling and vibration [16]–[19]. The mathematical modeling is done by Lagrange equation, the drilling vibration stability [20] and control method of the drill bit [21] are analyzed, and the correctness is verified by experiments [22]. However, the structure and guiding mechanism of the underwater mud-penetrator drill bit are different, and the Lagrangian modeling method is not clear enough to describe the specific force change and motion law of the drill bit during the guiding drilling process, the Newton Euler dynamics method needs further research to clarify the entire guiding process of the drill bit considering the nonlinear coupling interaction between drill bit, drill pipe and seabed geology.

In addition, the wear characteristics of the drill bit are also studied, which has reference significance for its structural design [23], [24] and material selection [25], [26]. Studying the guiding mechanism, statics and dynamics of underwater mud-penetrator drill bits, all in order to precisely control the drill bit [27]–[32] by adjusting the electro-hydraulic drive system of the non-excavation drilling rig [33]–[35] to match our pre-designed drill bit moving trajectory.

Within this paper, the guiding mechanism of the drill bit is analyzed according to its structure shape, discussing the interaction force between drill bits, drill pipe and seabed geology, and establishing the drill bit guiding dynamic model considering drill pipe stiffness and varying soil resistance by using the Newton-Eulerian dynamics method. By establishing the model, the direction change of the drill bit movement can be completed, thereby controlling the threading trajectory to conform to the optimal trajectory determined according to the seabed geological conditions. And we can have a clear grasp of the trajectory law and mechanical properties of the drill bit when guiding, the mathematical model was simulated by MATLAB/SIMULINK to verify its correctness, the obtained results fully reflect the force condition and motion law of the drill bit during the guiding process, which can be used as a reference for the control of the trajectory of the non-excavation drill bit, and also has reference significance for improving the guiding ability.

II. DRILL GUIDING PRINCIPLE

There are two working states when the underwater mud-penetrator is used to thread steel wire: the drill bit only advances but does not rotate, and the obtained threading trajectory is a curve; the drill bit advances and rotates, and the obtained trajectory is a straight line. This paper aim at the steering process dynamic model of the drill bit under the action of propulsive force, and the working principle of the drill guiding process is shown in Fig. 2.

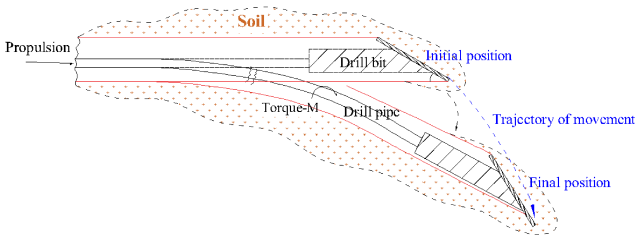

FIGURE 2. Drill guiding principle.

Under the action of the propulsive force, the drill bit will translate downward along the guiding plate, as the soil depth of the drill bit increases, the soil resistance increases. When the propulsion force is less than the soil resistance, the translation speed of the drill bit is reduced to zero, and the equilibrium state of the translational motion is reached. As the translational movement of the drill bit progresses, the drill pipe will deform and generate the torque, and the sum of the rotational torque generated by the deformed drill pipe and the propulsion torque is greater than that of the soil resistance torque, the drill bit begins to rotate. At this time, the soil extrusion force appears in the form of an additional rotational resistance moment and increases as the soil deformation increases, Moreover, due to the rotation of the drill bit, the deformation rate of the drill pipe is reduced, it reduces the torque of the drill pipe, when the rotational torque is less than the rotational resistance torque, the rotational speed of the drill bit is reduced to zero and reaching the equilibrium state of rotation. The state of the motion at the beginning and end is shown in Fig. 2.

The essence of this movement is the nonlinear coupling interaction between drill bit, drill pipe and seabed geology, the time during which the translational and rotational motion of the drill bit overlaps is related to the propulsive force,

the stiffness of the drill pipe, the connection mode of the drill pipe and the properties of the soil itself, such as the internal friction angle. As can be seen from Fig. 2, the maximum angle of rotation of the drill bit is limited by the drill guiding angle and the drill pipe.

III. MATHEMATICAL MODELING FOR GUIDING SYSTEM

A. BASIC ASSUMPTIONS

1) The soil has a uniform distribution and does not collapse after the drill bit is drilled into the hole;

2) The drill bit motion is a two-dimensional plane during a single guiding process, so the space guiding process is simplified into a multi-stage two-dimensional plane guiding process;

3) The drill pipe is continuous and guaranteed to be applied stable bit propulsion.

B. KINEMATIC MODELING

In this paper, we study the dynamics modeling of drill bit guidance and establish two right-handed coordinate systems: one is a fixed coordinate system (referred to as ''fixed system''), also called inertial coordinate system, fixed to the Earth; the other one is the motion coordinate system (referred to as ''moving system''), also called the following coordinate system, fixed to the drill bit, moving with the drill bit, the coordinate system is established as shown in Fig. 3.

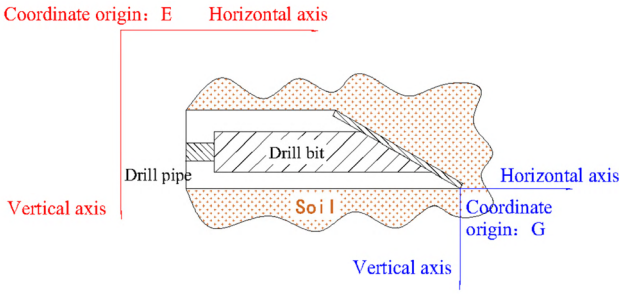

FIGURE 3. Drill bit coordinate system.

Fixed coordinate system $E-\xi\eta\zeta$ which is the inertial coordinate system fixed on the earth, used to determine the position, velocity and posture of the drill bit in the fixed system; the motion coordinate system *G-xyz* that is fixed on the drill bit and moves with the drill bit, and can represent the six degree freedom movement of the drill bit when it is threaded in the soil under the seabed shipwreck.

The coordinates (ξ, η, ζ) of the origin G of the following coordinate system in a fixed coordinate system, real-time indicates the specific position of the drill bit during the threading, the speed and acceleration of the drill bit under the fixed system; the angle value (ϕ, θ, ψ) of the fixed coordinate system relative to the following coordinate system indicates the real-time posture angle of the drill bit during the drilling process. Through the transformation, the real-time angle, the angular velocity and the angular acceleration of the drill bit in the inertial coordinate system are known. The parameters are defined as shown in Table 1 and Table 2 [36]–[39].

TABLE 1. Related parameters of drill bit in fixed coordinate system.

Parameter	ξ Axis	η Axis	ζ Axis
position	ξ	η	ζ
angle	ϕ	θ	ψ

TABLE 2. Related parameters of drill bit in motion coordinate system.

Parameter	x Axis	y Axis	z Axis
position	x	y	z
angle	θx	θy	θz
line speed	u	v	w
angular velocity	p	q	r
external force along the axis	X	Y	Z
torque along the shaft	K	M	N

The description of the spatial motion of the drill bit when the drilling is generally expressed by the Euler angle method, the coordinate transformation relationship of the moving coordinate system of the drill bit to the fixed coordinate system is related to the three posture angles ϕ, θ, ψ of the drill bit, so the following state quantity is defined. The position and posture vector of the drill bit under the fixed system is:

$$\eta = \begin{bmatrix} \eta_1^T & \eta_2^T \end{bmatrix}^T \eta_1 = \begin{bmatrix} \xi & \eta & \zeta \end{bmatrix}^T \eta_2 = \begin{bmatrix} \phi & \theta & \psi \end{bmatrix}^T \quad (1)$$

The linear velocity and angular velocity vector of the drill bit under the dynamic system are:

$$v = \begin{bmatrix} v_1^T & v_2^T \end{bmatrix}^T v_1 = \begin{bmatrix} u & v & \omega \end{bmatrix}^T v_2 = \begin{bmatrix} p & q & r \end{bmatrix}^T \quad (2)$$

The force and torque of the drill bit under the dynamic system are:

$$\begin{aligned} \tau &= \begin{bmatrix} \tau_1^T & \tau_2^T \end{bmatrix}^T \tau_1 = \begin{bmatrix} \tau_X & \tau_Y & \tau_Z \end{bmatrix}^T \tau_2 \\ &= \begin{bmatrix} \tau_K & \tau_M & \tau_N \end{bmatrix}^T \end{aligned} \quad (3)$$

1) LINEAR VELOCITY CONVERSION MATRIX

The conversion equation of the drill bit at the speed of the fixed line to the speed of the moving system is as follows:

$$v_1 = J_1(\eta_2)^{-1}\dot{\eta}_1 \quad (4)$$

where $J_1(\eta_2)^{-1}$ is the speed conversion matrix, which can usually be obtained by three rotation transformations around the coordinate axis (5), as shown at the bottom of the next page.

Through this matrix, the velocity of the system can be expressed by the fixed physical quantity:

$$\begin{cases} u = \cos\theta \cdot \dot{\xi} - \sin\theta \cdot \dot{\zeta} \\ w = \sin\theta \cdot \dot{\xi} + \cos\theta \cdot \dot{\zeta} \end{cases} \tag{6}$$

2) ANGULAR VELOCITY CONVERSION MATRIX

The angular velocity conversion matrix of the angular velocity of the drill bit on the fixed coordinate system to the following coordinate system is:

$$v_2 = J_2(\eta_2)^{-1}\dot{\eta}_2 \tag{7}$$

where $J_2(\eta_2)^{-1}$ is the transformation matrix from the fixed system to the moving system.

$$J_2(\eta_2)^{-1} = \begin{bmatrix} 1 & 0 & -\sin\theta \\ 0 & \cos\phi & \cos\theta\sin\phi \\ 0 & -\sin\phi & \cos\theta\cos\phi \end{bmatrix} \tag{8}$$

Through this transformation matrix, the angular velocity of the moving system can be expressed by the fixed physical quantity:

$$\begin{cases} q = \dot{\theta} \\ \dot{q} = \ddot{\theta} \end{cases} \tag{9}$$

C. DRILL GUIDING DYNAMICS MODELING

1) THE FORCE ANALYSIS

The threading movement process of the underwater guiding drill bit is very complicated, the precise study of this process needs to fully consider the nonlinear coupling between the drill bit, the drill pipe and the seabed geology, and also needs to clarify the other interference that the drill bit receives when guiding, only in this way can a realistic nonlinear dynamic model be established. Firstly, the force analysis of the drill bit is completed, and the influence of the interaction between the drill bit and the surrounding soil under the action of the force is clarified.

Soil mechanics foundation: The soil reaches the limit equilibrium state, at the time, the ratio of the maximum and minimum principal stress of the plane principal stress is a certain value, and the magnitude of the ratio is determined by the internal friction angle φ of the soil and the C adhesion coefficient [40], [41].

$$K_p = \frac{\sigma_{\max}}{\sigma_{\min}} = \tan^2(45^\circ + \frac{\varphi}{2}) \tag{10}$$

where K_p is the soil pressure coefficient, σ_{max} and σ_{min} are the maximum and minimum principal stress.

For the static analysis of the drill bit, the force synthesis chart is shown in Fig. 4.

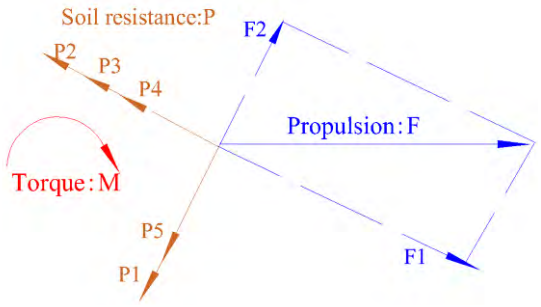

FIGURE 4. Drill force analysis.

1) Passive soil pressure $\sigma_{\max}$ acting on the front side of the guiding plate, the resistance formed is P_1, the axial component resistance is P_{1x}, and the vertical component resistance is P_{1z} [41], [42].

Force size:

$$P_1 = \int_0^h \sigma_{max}\mathrm{d}y = (\gamma H_0 K_\mathrm{p} 2C\sqrt{K_\mathrm{p}})LB \tag{11}$$

where L and B is the guiding plate length and width, γ is the soil severity, C is the cohesion of the soil, and α is the guiding angle.

2) The soil rises along the guiding plate, and the frictional resistance generated by the blade is P_2, the axial component resistance is P_{2x}, and the vertical component resistance is P_{2z}.

Force size:

$$P_2 = \frac{LB\mu}{\cos^2\alpha}[\gamma H_0(K_\mathrm{p}+3\tan\varphi)+2C\sqrt{K_\mathrm{p}}) \tag{12}$$

where$\mu$is the friction coefficient of soil and steel, φ is the friction angle of soil.

3) Passive soil pressure $\sigma_{\max}$ acting on the side face of the guiding plate, the resistance formed is P_3, the axial component resistance is P_{3x}, and the vertical component resistance is P_{3z}.

Force size:

$$P_3 = (\gamma H_0 K_\mathrm{p} 2C\sqrt{K_\mathrm{p}})Bh \tag{13}$$

where h is the thickness of the blade.

4) The propulsive force F formed by the non-excavation drilling rig hydraulic system acting on the drill bit has an axial component of F and a vertical component of 0.

5) The resistance generated by the soil pressing force generated by the guiding process is P_4 and P_5, the two are respectively the soil pressing force generated by the translational and rotational movement of the drill bit, the axial component resistance is P_{4x} and P_{5x}, and the vertical component

$$J_1(\eta_2)^{-1} = \begin{bmatrix} \cos\theta\cos\psi & \cos\theta\sin\psi & -\sin\theta \\ \cos\psi\sin\theta\sin\phi - \cos\phi\sin\psi & \cos\phi\cos\psi + \sin\phi\sin\theta\sin\psi & \cos\theta\sin\phi \\ \sin\phi\sin\psi + \cos\phi\sin\theta\cos\psi & \cos\phi\sin\theta\sin\psi - \cos\psi\sin\phi & \cos\phi\cos\theta \end{bmatrix} \tag{5}$$

resistance is P_{4z} and P_{5z}.

$$P_4 = k_1 f(S^3) + k_2 f(S^2) + k_3 f(S) \tag{14}$$
$$P_5 = k_1 f(\theta^2) + k_2 f(\theta) \tag{15}$$

where S is the translation distance of the drill bit, θ is the rotation angle of the drill bit, k_1, k_2 and k_3 are constant. When the drill bit is subjected to horizontal and rotary motions under the action of propulsion, the seabed geology can be regarded as being squeezed in two directions, and the soil will be deformed to generate a nonlinear soil resistance to react to the drill bit, and the two interact and influence each other.

6) The torque M generated by the deformation of the drill pipe is related to the stiffness, deformation rate and drill pipe connection method. Torque and propulsion torque act on the drill bit to rotate, and in the process of rotation, it is always affected by the opposite effect of soil resistance until it reaches a state of stress balance, the interaction between the three causes the drill bit to complete the guiding process.

The soil extrusion force increases with the increase of soil deformation, which is related to the penetration distance, rotation angle, soil friction angle and Poisson's ratio of the drill bit, and the application of the drill guiding angle will decompose the propulsion force and the soil resistance along the axial direction and perpendicular to the axial direction can be obtained:

$$\begin{aligned}\tau_x &= F - P_{1x} - P_{2x} - P_{3x} - P_{4x} - P_{5x} \\ &= F - P_1 \sin\alpha - P_2 \cos\alpha - P_3 \cos\alpha - P_4 \cos\alpha - P_5 \sin\alpha\end{aligned} \tag{16}$$

$$\begin{aligned}\tau_z &= P_{1z} - P_{2z} - P_{3z} - P_{4z} + P_{5z} \\ &= P_1 \cos\alpha - P_2 \sin\alpha - P_3 \sin\alpha - P_4 \sin\alpha + P_5 \cos\alpha\end{aligned} \tag{17}$$

where τ_M is the torque around the y axis, when the drill bit only advances and does not rotate, under the action of the propulsive force F, it will rotate a certain angle around point G in the Fig. 3, re-adjust the posture of the guiding plate and the movement direction of the drill bit, thereby controlling the drilling trajectory to match the pre-designed optimal trajectory of the design, and completing the task of changing the drilling direction of the drill bit. τ_M can be obtained from the above -mentioned resistance, propulsive force and torque M generated by the deformation of the drill pipe. According to the size of the drill bit defined in the AutoCAD diagram, the counterclockwise torque is positive value and the clockwise torque is negative value.

$$\begin{aligned}\tau_M = -F \times \frac{L}{2} - \mathrm{M} + P_1 \times \frac{L}{2} + P_2 \times h + P_3 \\ \times \frac{h}{2} + P_4 \times \frac{h}{2} + P_5 \times \frac{L}{2}\end{aligned} \tag{18}$$

2) DRILL GUIDING DYNAMICS

Assuming that the drill bit is a rigid body, the Newton's motion equation of the rigid body can be expressed as follows [43]–[45]:

$$m[\dot{v}_1 + v_2 \times v_1 + \dot{v}_2 \times r_G + v_2 \times (v_2 \times r_G)] = \tau_1 \tag{19}$$
$$I_0 \dot{v}_2 + v_2 \times (I_0 v_2) + m r_G \times (\dot{v}_1 + v_2 \times v_1) = \tau_2 \tag{20}$$

where m is the drill bit quality, $r_G = (x_G, y_G, z_G)^T$ is the barycentric coordinates of the drill bit in the motion coordinate system, τ_1 and τ_2 are the external force and external torque, I_0 is the drill bit moment of inertia matrix.

Firstly, the steering of the drill bit in the two-dimensional plane is studied, and then the rotation of the drill bit is applied to the guidance of the drill bit in the three-dimensional space, and it is assumed that the center of gravity of the drill bit does not coincide with the origin of the following coordinate system. Therefore, the above formula can be simplified.

$$\begin{cases} m(\dot{u} + wq - x_G q^2 + z_G \dot{q}) = \tau_x \\ m(\dot{w} - uq - z_G q^2 - x_G \dot{q}) = \tau_z \\ I_y \dot{q} + m[z_G(\dot{u} + \mathrm{qw}) - x_G(\dot{w} - qu)] = \tau_M \end{cases} \tag{21}$$

In the following coordinate system, the angular velocity can be converted into the physical quantity in the inertial coordinate system by the transformation matrix, and Eq. (6)-Eq. (9) can be substituted into the above Euler dynamics formula.

Suppose x_1 is the position ξ of the drill bit in the fixed coordinate system in the soil, x_2 is the position ζ, x_3 is the speed v_ξ moving along the ξ axis, x_4 is the speed v_ζ moving along the ζ axis, and x_5 is the angle θ around the η rotation, x_6 is the angular velocity q around the rotation of η.

Simplify the drill guiding dynamics model:

$$\begin{aligned}\dot{x}_1 &= x_3 \\ \dot{x}_2 &= x_4 \\ \dot{x}_3 &= \frac{\tau_x}{m}\cos x_5 + \frac{\tau_z}{m}\sin x_5 - x_4 x_6 - x_6^2(x_G \cos(x_5) \\ &\quad + z_G \sin(x_5)) + \dot{x}_6(z_G \cos(x_5) - x_G \sin(x_5)) \\ \dot{x}_4 &= \frac{\tau_z}{m}\cos x_5 - \frac{\tau_x}{m}\sin x_5 + x_3 x_6 \\ &\quad + x_6^2(x_G \sin(x_5) - z_G \cos(x_5)) - \dot{x}_6(x_G \cos(x_5) + z_G \sin(x_5)) \\ \dot{x}_5 &= x_6 \\ \dot{x}_6 &= \frac{\tau_M}{I_y} \\ &\quad + m\frac{x_G(\sin(x_5)\dot{x}_3 + \cos(x_5)\dot{x}_4 - \cos(x_5)x_3 x_6 + \sin(x_5)x_4 x_6)}{I_y} \\ &\quad - m\frac{z_G(\cos(x_5)\dot{x}_3 - \sin(x_5)\dot{x}_4 + \sin(x_5)x_3 x_6 + \cos(x_5)x_4 x_6)}{I_y}\end{aligned} \tag{22}$$

where τ_x, τ_z, τ_M is substituted by Eq. (16), Eq. (17) and Eq. (18) respectively, the $\dot{x}_3\dot{x}_4$ and $\dot{x}_6$ three equations simplification can be used to obtain the drill guiding dynamic model, if the center of gravity of the drill bit is at the coordinate origin($x_G = z_G = 0$), then the kinetic equation can be obtained by simplification formula Eq. (22).

IV. SIMULATION ANALYSIS

A. DRILL GUIDING PROCESS RESULTS

The geological conditions: Soil cohesion is $15000P_a$, Soil severity is 19000N/m^3, soil internal friction angle is 19°, soil pressure coefficient is $K_p = 1$, guiding plate angle is 30°, propulsion is 3000N.

The drill bit guiding motion diagram is drawn by integrating the abscissa, ordinate and rotation angle of the drill bit. The simulation result is shown in Fig. 5. The position coordinates of the drill bit at any time can be known, Through the angle change of $A_1\,A_2\,A_3\,A_4$, the rotation angle of the drill bit at every moment and the threading direction of the next stage can be known.

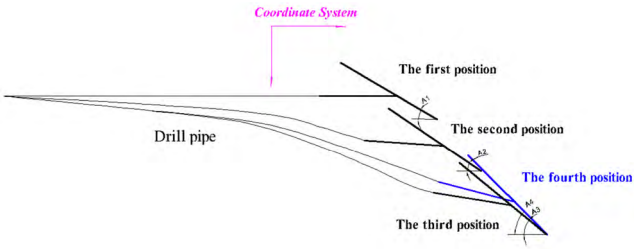

FIGURE 5. Drill guiding motion diagram.

The specific movement situation: The drill bit begins with the resultant motion that is synthesized along the translation of the guiding plate and the rotation around the coordinate axis. When the drill bit is moved to a certain depth, the translation stops, and the drill bit is deflected by a small angle with respect to the initial position, the drill pipe begins to bend and deform, generating a torque M, and then the drill bit rotates under the influence of propulsive force and drill rod torque, when the rotation reaches a certain angle, the rotation stops. In the process, the rotation angle of the drill bit is significantly increased with the previous process, and the deflection guidance of the drill bit mainly comes from this process.

B. GEOLOGICAL CHANGE INFLUENCE RESULTS

Under the condition that the propulsion force is un-changed at 3000*N*, when the geological change from soft to hard, we can know the influence of geological change on the translational and rotational guidance of the drill bit. For the translation we choose the soil resistance as the research object, for the rotation we choose rotational angular velocity as the research object. Simulation results is showed in Fig. 6 and Fig. 7.

It can be seen from Fig. 6 and Fig. 7 that as the drill bit is drilled and rotated, the depth of the soil is increasing, and the soil resistance is continuously increased, the soil pressure on the front of the guiding plate is 1412N, which is the dominant part of the resistance, and it starts to increase from 1225N, the largest increase, the blade friction is 387N, the value is small and the increase is not big. When the seabed geology changes suddenly in 0.2s, that is, from soft to hard, for the translation, the threading speed of the drill bit

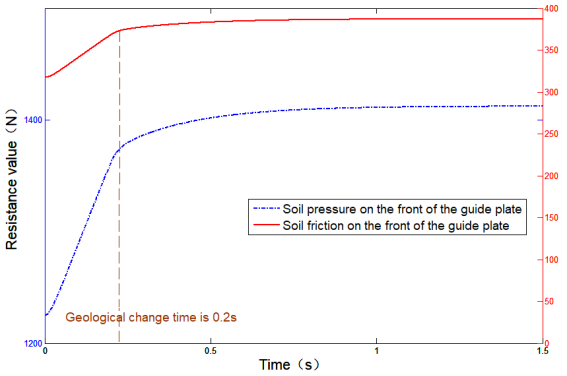

FIGURE 6. Simulation curve of influence of geological mutation on soil resistance.

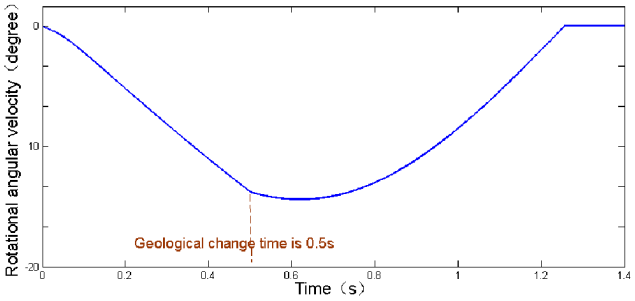

FIGURE 7. Simulation curve of geological mutation on the rotational angular velocity of the drill bit.

decreases, and the soil depth increases per unit time, resulting in a decrease in the resistance growth rate, the time required to reach the bit balance state is reduced. When the seabed geology changes in 0.5s, the rotational resistance torque of the bit rotation significantly increase for the rotation, and the decrease in angular acceleration results in a decrease in the angular velocity growth rate. In order to obtain the best drill guiding effect, we should explore the actual seabed geology of the shipwreck in advance and design the optimal trajectory of the drill bit threading wire to prevent the geological change from causing the drill to vibrate, thus affecting its guiding effect.

C. DRILL GUIDING ANGLE INFLUENCE RESULTS

The geological and propulsive conditions are the same as ***A***. Using the *pi*/4, *pi*/6, *pi*/10 guiding angle drill bit to study the influence of different steering angles on the rotation guiding ability. The simulation results are shown in Fig. 8.

It can be seen from Fig. 8 that in the case of the same seabed geology with the same propulsive force, with the decrease of the soil guiding angle, the rotation angles of the drill bits are 15.6°, 18.3°, 20.6°, it respectively increased, and the guiding ability is enhanced. Time the drill guiding angle decreases *pi*/12-*pi*/15, the angle increases 2°-3°, and within a certain range, the two are proportional. It is necessary to design the drill with the optimal guiding angle according to the actual

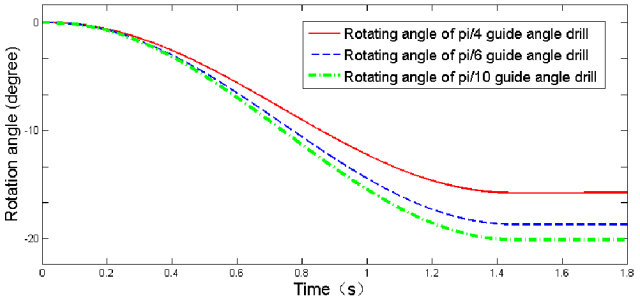

FIGURE 8. Simulation curve of the rotation angle of different guiding angle drill bits.

working conditions, so as to better control the drill guiding so as to basically conform to the optimal trajectory designed.

D. PROPULSION INFLUENCE RESULTS

Under the same geological conditions, the propulsive force of 2500N, 3000N, 3500N was applied to the drill bit to study the influence of the drill movement law, guiding ability and force variation. The specific simulation results are shown in Fig. 9–Fig. 12.

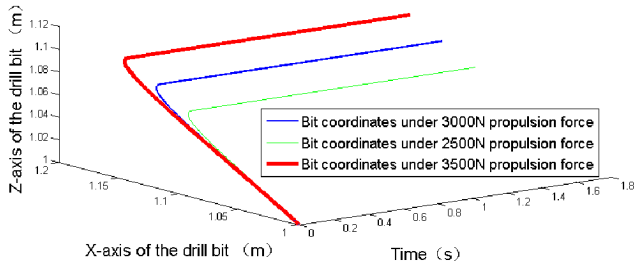

FIGURE 9. Simulation curve of drill bit space trajectory under different propulsive forces.

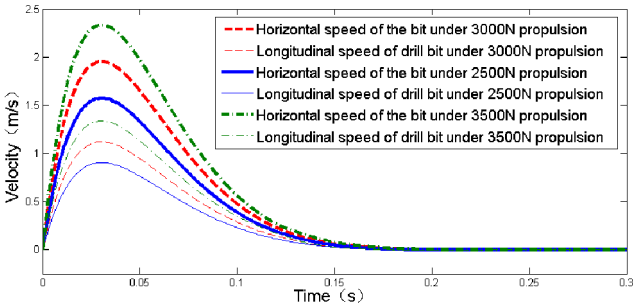

FIGURE 10. Simulation curve of drill bit speed under different propulsive forces.

It can be seen from the results that as the propulsive force of the drill bit increases, the initial acceleration and the angular acceleration become larger, so that the translation distance and the rotation angle increase continuous, and the translation distance X is 11.2cm, 14.1cm, 16.8cm respectively, the translation distance Z is 6.5cm, 8.2cm, 9.5cm, the maximum horizontal velocity is 1.57m/s, 1.95 m/s, 2.33m/s, the maximum vertical velocity is 0.90m/s, 1.13m/s, and 1.33m/s respectively.

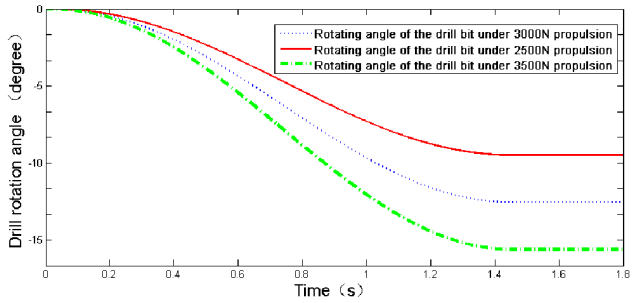

FIGURE 11. Simulation curve of drill bit rotation angle under different propulsive forces.

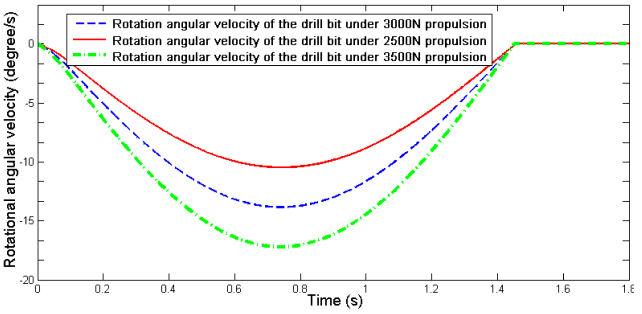

FIGURE 12. Simulation curve of drill bit rotation angular velocity under different propulsive forces.

As seen from the rotation angle diagram that the drill bit does not start to rotate immediately, as the drill bit moves along the guiding plate, the drill rod is deformed to generate a torque When the rotational torque formed by the propulsive force and M is greater than the rotational resistance torque, the drill bit begins to rotate, As the soil extrusion deformation increases and the depth of the bit increases, the soil resistance increases continuously, and the acceleration and angular acceleration decrease first and then increase in the opposite direction until the equilibrium state of zero speed and angular velocity is reached. At this time, the rotation angle of the drill bit is 9.5° ,12.5°, 15.8°respectively, the maximum rotational angular velocity is 10.4 degree/s,13.5 degree /s,17.2 degree /s, for every 500N increase in propulsion, the angle increases 3° and it is the proportional relationship between the two within a certain range.

Different propulsive forces produce different coupling effects; Therefore, the propulsion force should be reasonably applied to guide the rotation of the drill bit, and the monitoring device is used to monitor the progress of the entire guiding process, the time during which the translational motion of the drill bit overlaps with the rotational motion is related to the magnitude of the propulsive force [46], the stiffness of the drill pipe and the soil properties of the seabed.

E. DIFFERENT GEOLOGY RESULTS

In the simulation, soft seabed geology: soil cohesion is $C = 2000\mathrm{P_a}$, internal friction angle is 36°, middle seabed geology: is $C = 50000\mathrm{P_a}$, internal friction angle is 25°, hard

seabed geology: soil cohesion is $C = 100000\mathrm{P_a}$, internal friction angle is 16°.

In different geological conditions of the seabed, 3500N propulsion force is applied to the drill bit to study the influence of the drill bit on the threading distance and the rotation angle, as is shown in Fig. 13 and Fig. 14.

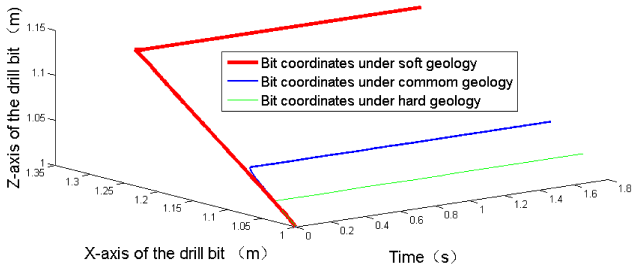

FIGURE 13. Simulation curve of drill bit space trajectory under different geology.

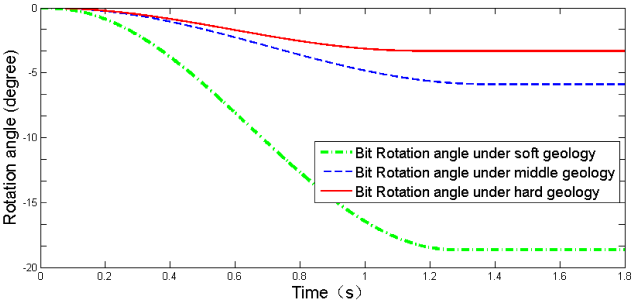

FIGURE 14. Simulation curve of drill bit rotation angle under different geology.

It can be seen from Fig. 13 and Fig. 14 that under the same propulsive force, as the geology becomes harder, the soil resistance becomes larger, so that the initial acceleration and the angular acceleration are smaller, the moving distance and the rotation angle of the drill bit is reduced, and the translation distance X is 27.3cm, 8.4cm, and 3.7cm respectively, the translational distance Z is 13.0cm, 4.8cm, and 2.2cm respectively, the hardening of the geology also causes the drill bit to reach an equilibrium state with zero speed and zero angular velocity earlier, in this time, the angles is 19.2° ,5.8°, 3.3°. For the first 48000 $\mathrm{P_a}$ soil cohesion changes, the rotation angle changes 13.4°, and the next 50000 $\mathrm{P_a}$ soil cohesion changes, the rotation angle changes 2.5°, it is known that the bit deflection angle is more sensitive to softer geological changes.

The drill bit threads in different geometries, which creates the different coupling effects between the drill bit, the drill pipe and the soil. Therefore, in designing the optimal trajectory of the drill bit to thread steel wire, it is necessary to explore the geological conditions of the seabed, so that the drill trajectory is as far as possible in the soft seabed geology [47], improve the guiding ability of the drill bit, only in this way can the drill be controlled more easily and the work efficiency is improved.

F. DIFFERENT GUIDING PLATE AREA RESULTS

Under different guiding plate area, apply 3000N propulsive force to the drill bit, and study the movement process of the drill bit such as: threading distance and rotation angle and angular velocity, guiding ability, and force variation. The area of the drill guiding plate is $0.00625\mathrm{m^2}$ $0.0125\mathrm{m^2}$ $0.025\mathrm{m^2}$ $0.0375\mathrm{m^2}$ $0.05\mathrm{m^2}$, the research result is shown in Fig. 15–Fig. 17.

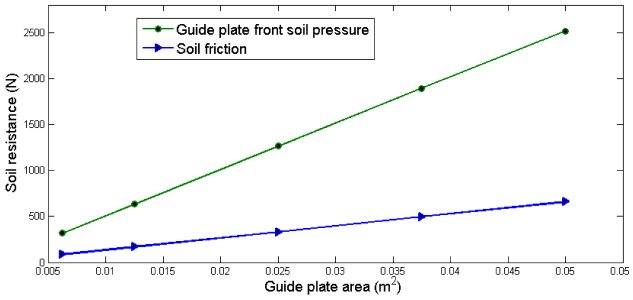

FIGURE 15. Soil resistance of the drill bit under different guiding plate areas.

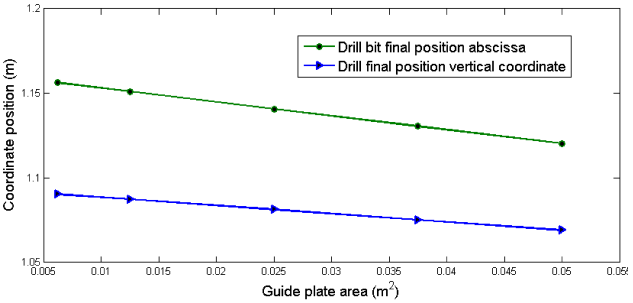

FIGURE 16. Position coordinates of the drill bit under different guiding plate areas.

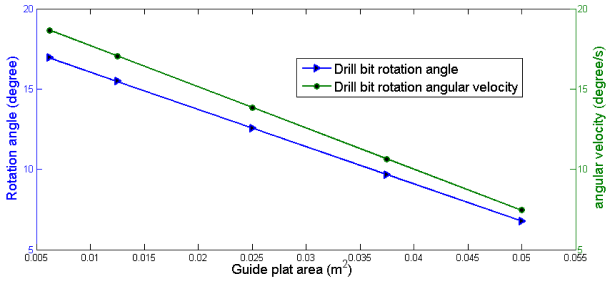

FIGURE 17. Rotation parameters of drill bit under different guiding plate areas.

According to the analysis of the Fig. 15–Fig. 17, as the area of the drill guiding plate increases, the soil resistance and friction force of the drill bit increase continuously, the maximum soil resistance is 316.9N 633.3N 1263.7N 1891.2N 2515.7N, the maximum friction force is 83.3N 166.4N 331.7N 496.1N 659.2N respectively. Due to the increase of soil resistance, the horizontal moving distance and the vertical moving distance of the drill bit are reduced, and the horizontal moving

distance is 0.156m 0.151m 0.141m 0.131m 0.120m, the vertical moving distance is 0.090m 0.087m 0.081m 0.075m 0.069m respectively. The rotating resistance torque of the drill bit is increased, so the rotation angle is decreased, the guiding ability is decreased, and the angle values are 16.9° 15.4° 12.6° 9.6° 6.7° respectively.

The difference in the area of the guiding plate causes the difference in the structure of the drill bit, which in turn causes the coupling between the drill bit, the drill pipe and the soil to be different, so that the drill guiding ability changes. The area of the guiding plate has a great influence on the guiding ability of the drill bit, the area of the guiding plate is twice the original, and the reduction of the drill bit rotation angle is also doubled. Therefore, in order to ensure the guiding ability of the drill bit, it is necessary to reasonably reduce the area of the guiding plate so that the drill bit can rotate as many angles as possible under the same propulsive force, but the strength requirements of the structure and the actual work requirements need to be met [48].

G. THREE-DIMENSIONAL SPACE DRILLING TRAJECTORY

By changing the posture of the guiding plate in three-dimensional space by the rotation of the drill bit, and applying the above dynamic modeling formula, the dynamic modeling and rotation guidance of the drill bit in three-dimensional space can be realized.

V. CONCLUSION

In this paper, the nonlinear dynamic model of underwater mud-penetrator under varying soil resistance is firstly established by Newton's Euler dynamic equation, and the simulation results are analyzed help to describe the movement of the steering process of drill bit. The research work lay a foundation for the precise threading trajectory control of underwater mud-penetrator. Related conclusions are as follows:

1) The guiding process of underwater mud-penetrator can be regarded as the resultant movement of the drill bit along the guiding plate and the rotation around the coordinate axis. The specific overlap time of the two movements is connected with the propulsion force, the drill pipe stiffness and the seabed soil etc. The essence of the drill bit rotation is that the superposition of the propulsion torque and the deformation torque of the drill pipe is greater than soil resistance torque, the maximum value of the rotation angle is related to a number of factors, such as drill pipe stiffness, drill guiding angle, propulsion and subsea soil properties.

2) The deflection angle of the drill bit can be regarded as proportional to the guiding angle and propulsion force within a certain range, for each *pi*/12-*pi*/15 reduction of the drill bit guiding angle, the deflection angle is increased by 2°-3°, for each 500*N* increase in propulsion, the deflection angle of the drill bit is increased by 3°. The area of the guiding plate has a great influence on the guiding ability of the drill bit, the area of the guiding plate is twice the original, the reduction of the drill bit rotation angle is also doubled. In addition, the deflection angle of the drill bit is more sensitive to softer geological changes, with the soft geological and hard seabed geology of the same variation range, the deflection angle of the drill bit is more obvious under soft geological conditions.

3) Before the non-excavation drilling rig is used to thread steel wire, firstly explore the seabed geological conditions, design the optimal trajectory of the drill bit to thread wire. Then design the drill bit structure with different guiding angles, so as to have different guiding ability. Use the appropriate material and connection method of the drill pipe according to working conditions, thereby maximally increasing the rotational torque of the drill bit. Finally use the appropriate size of propulsion according to the geological conditions and simulation results. The above measures can give full play to the guiding ability of the drill bit.

ACKNOWLEDGMENT

The authors thank the reviewers for their elaborate and incisive suggestions.

REFERENCES

[1] F. Soreide and M. E. Jasinski, "Ormen lange: Investigation and excavation of a shipwreck in 170 m depth," in *Proc. OCEANS MTS/IEEE*, Washington, DC, USA, Sep. 2005, pp. 2334–2338.
[2] S. November, K. Smith, and J. Edgar, "ARS-50 CLass salvage ship—Super salvor," in *Proc. OCEANS*, San Francisco, CA, USA, 1983, pp. 1078–1081.
[3] V. Paka, N. Rimski-Korsakov, and V. Smirnov, "Ship wrecks exploration," in *Proc. IEEE US/EU Baltic Int. Symp.*, Klaipeda, Lithuania, May 2006, p. 1.
[4] C. De Moustier *et al.*, "Tools and techniques for deep water sediment sampling around a ship wreck," in *Proc. Int. Symp. Underwater Technol.*, Tokyo, Japan, 1998, pp. 7–10.
[5] C. Bartholomew, A. Rynecki, and D. Saveker, "Underwater explosive cutting in ship salvage," in *Proc. Conf. OCEAN*, San Diego, CA, USA, 1975, pp. 592–596.
[6] A. Salmi, J. Eskelinen, M. Peura, E. Hæggström, K. Steffen, and L. Montonen, "Non-destructive evaluation of the 18th century ship wreck Vrouw Maria," in *Proc. IEEE Int. Ultrason. Symp.*, Rome, Italy, Sep. 2009, pp. 1479–1482.
[7] K. Yang, T. Ge, and X. Y. Wang, "Research on attitude and position tracking algorithm of drill bit for underwater mud-penetrator," *Adv. Mater. Res.*, vols. 591–593, pp. 1381–1385, Nov. 2012.
[8] K. Yang, T. Ge, and X. Y. Wang, "Attitude tracking and location algorithm of drill bit for underwater mud-penetrator," *Appl. Mech. Mater.*, vol. 203, no. 6, pp. 395–400, Oct. 2012.
[9] Y. Hui, G. E. Tong, Y. Ke, and X. Y. Wang, "Research on Attitude Measuring Method of Bit in Underwater Mud-Penetrator," *J. Shanghai Jiaotong Univ.*, vol. 46, no. 3, pp. 446–450, 2012.
[10] X. Song, M. Vadali, Y. Xue, and J. D. Dykstra, "Tracking control of rotary steerable toolface in directional drilling," in *Proc. IEEE Int. Conf. Adv. Intell. Mechatronics (AIM)*, Banff, AB, Canada, Jul. 2016, pp. 1210–1215.
[11] Y. Sun, Q. Di, W. Zhang, W. Chen, Y. Yang, and J. Zheng, "Dynamic inclination measurement at-bit based on MEMS accelerometer," in *Proc. 29th Chin. Control Decision Conf. (CCDC)*, Chongqing, China, 2017, pp. 5016–5019.
[12] Z.-Y. Liao, Z.-Z. Liang, Y.-F. Yang, W. Yan, and C.-A. Tang, "Numerical simulation of fragmentation process of jointed rock mass induced by a drill bit under dynamic loading," *Chin. J. Geotech. Eng.*, vol. 35, no. 6, pp. 1147–1155, 2013.
[13] Y.-F. Yang, Z.-Z. Liang, and C.-A. Tang, "Rock fragmentation mechanism induced by a drill bit subjected to dynamic loading," *Rock Soil Mech.*, vol. 34, no. 6, pp. 1775–1785, 2013.
[14] E. Sharapov, X. Wang, and E. Smirnova, "Drill bit friction and its effect on resistance drilling measurements in logs," in *Proc. 20th Int. Nondestruct. Testing Eval. Wood Symp.*, Madison, WI, USA, 2017, pp. 405–415.
[15] J. Hu, Z. Zhang, Y. Guo, and L. Li, "Research on cutting resistance torque of soil in auger drilling," in *Proc. ICDMA*, vol. 20, pp. 1047–1050, Jun. 2013.

[16] I. Mnafeg, A. Abichou, and L. Beji, "Analytical and numerical studies of sonic drillstring dynamics," in *Proc. 24th Medit. Conf. Control Automat. (MED)*, Athens, Greece, 2016, pp. 814–819.

[17] O. J. Hoffmann, J. R. Jain, R. W. Spencer, and N. Makkar, "Drilling dynamics measurements at the drill bit to address today's challenges," in *Proc. IEEE Int. Instrum. Meas. Technol. Conf.*, Graz, Austria, May 2012, pp. 443–448.

[18] Y. Wang, Q. Quan, H. Yu, H. Li, D. Bai, and Z. Deng, "Impact dynamics of a percussive system based on rotary-percussive ultrasonic drill," *Shock Vib.*, vol. 2017, Oct. 2017, Art. no. 5161870.

[19] L. Jiean, H. Can, W. Xufeng, W. Wei, and L. Xinying, "Study on ultrasonic vibration deep microspore drilling bit dynamic state," in *Proc. 5th Int. Conf. Intell. Syst. Design Eng. Appl.*, Hunan, China, 2014, pp. 989–992.

[20] S. Toumi, R. Mlayeh, L. Beji, and A. Abichou, "Stability analysis of oilwell drilling torsional vibrations," in *Proc. 26th Medit. Conf. Control Automat.*, 2016, pp. 677–682.

[21] T. Vromen *et al.*, "Mitigation of torsional vibrations in drilling systems: A robust control approach," *IEEE Trans. Control Syst. Technol.*, to be published.

[22] K. Yu, S. Iwata, K. Ohnishi, S. Usuda, T. Nakagawa, and H. Kawana, "Modeling and experimentation of drilling vibration for implant cutting force presenting system," in *Proc. 3th Int. Workshop Adv. Motion Control (AMC)*, Yokohama, Japan, 2014, pp. 711–716.

[23] Q. Quan, D. Bai, Z. Zhao, Z. Deng, H. Li, and Y. Wang, "Development of a rotary-percussive ultrasonic drill for extraterrestrial rock sampling," in *Proc. IEEE Int. Ultrason. Symp. (IUS)*, Washington, DC, USA, Sep. 2017, pp. 1–4.

[24] X. Li, P. Harkness, K. Worrall, R. Timoney, and M. Lucas, "A parametric study for the design of an optimized ultrasonic percussive planetary drill tool," *IEEE Trans. Ultrason., Ferroelectr., Freq. Control*, vol. 64, no. 3, pp. 577–589, Mar. 2017.

[25] E. Sharapov, X. Wang, E. Smirnova, and J. P. Wacker, "Wear behavior of drill bits in wood drilling resistance measurements," *Wood Fiber Sci. J. Soc. Wood Sci. Technol.*, vol. 50, no. 2, pp. 154–166, 2018.

[26] R. Y. Kuftyrev, N. I. Polushin, O. S. Kotel'Nikova, A. I. Laptev, and M. N. Sorokin, "Wear resistance of polycrystalline diamond cutters for drill bits," *Steel Transl.*, vol. 47, no. 9, pp. 594–598, 2017.

[27] Z. Chen, B. Yao, and Q. Wang, "Accurate motion control of linear motors with adaptive robust compensation of nonlinear electromagnetic field effect," *IEEE/ASME Trans. Mechatronics*, vol. 18, no. 3, pp. 1122–1129, Jun. 2013.

[28] Z. Chen, B. Yao, and Q. Wang, "μ-Synthesis-based adaptive robust control of linear motor driven stages with high-frequency dynamics: A case study," *IEEE/ASME Trans. Mechatronics*, vol. 20, no. 3, pp. 1482–1490, Jun. 2015.

[29] Z. Chen, Y.-J. Pan, and J. Gu, "Integrated adaptive robust control for multilateral teleoperation systems under arbitrary time delays," *Int. J. Robust Nonlinear Control*, vol. 26, no. 12, pp. 2708–2728, Aug. 2016.

[30] M. Yuan, Z. Chen, B. Yao, and X. Zhu, "Time optimal contouring control of industrial biaxial gantry: A high-efficient analytical solution of trajectory planning," *IEEE/ASME Trans. Mechatronics*, vol. 22, no. 1, pp. 247–257, Feb. 2017.

[31] C. Li, C. Li, Z. Chen, and B. Yao, "Advanced synchronization control of a dual-linear-motor-driven gantry with rotational dynamics," *IEEE Trans. Ind. Electron.*, vol. 65, no. 9, pp. 7526–7535, Sep. 2018.

[32] W. Sun, S. Tang, H. Gao, and J. Zhao, "Two time-scale tracking control of nonholonomic wheeled mobile robots," *IEEE Trans. Control Syst. Technol.*, vol. 24, no. 6, pp. 2059–2069, Nov. 2016.

[33] W. Sun, H. Pan, and H. Gao, "Filter-based adaptive vibration control for active vehicle suspensions with electrohydraulic actuators," *IEEE Trans. Veh. Technol.*, vol. 65, no. 6, pp. 4619–4626, May 2016.

[34] J. Yao and W. Deng, "Active disturbance rejection adaptive control of hydraulic servo systems," *IEEE Trans. Ind. Electron.*, vol. 64, no. 10, pp. 8023–8032, Oct. 2017.

[35] J. Yao, W. Deng, and Z. Jiao, "RISE-based adaptive control of hydraulic systems with asymptotic tracking," *IEEE Trans. Automat. Sci. Eng.*, vol. 14, no. 3, pp. 1524–1531, Jul. 2015.

[36] Q. Yang, Q. Meng, J. Sun, and Z. Wang, "Design of move-in-mud robot and kinematics modeling," in *Proc. 5th World Congr. Intell. Control Automat.*, Hangzhou, China, 2004, pp. 4627–4630.

[37] R. E. G. Vargas, E. E. R. Vazquez, C. A. N. Martin, J. R. D. Fuentes, R. H. Alvarado, and H. G. Cuatzin, "An adaptation for a commercial ROV to inspect the bridges undermining on the Mexican rivers: Dynamic and kinematic modelling simplification and control," in *Proc. IEEE Int. Autumn Meeting Power, Electron. Comput.*, Nov. 2017, pp. 1–6.

[38] S. M. Savaresi, F. Previdi, A. Dester, S. Bittanti, and A. Ruggeri, "Modeling, identification, and analysis of limit-cycling pitch and heave dynamics in an ROV," *IEEE J. Ocean. Eng.*, vol. 29, no. 2, pp. 407–417, Apr. 2004.

[39] Y. Ke, W. Xuyang, G. Tong, and W. Chao, "A dynamic model of ROV with a robotic manipulator using Kane's method," in *Proc. 5th Int. Conf. Meas. Technol. Mechatronics Automat.*, Hong Kong, 2013, pp. 9–12.

[40] M. Fernandes and C. Cook, "Drilling of carbon composites using a one shot drill bit. Part I: Five stage representation of drilling and factors affecting maximum force and torque," *Int. J. Mach. Tools Manuf.*, vol. 46, no. 1, pp. 70–75, 2006.

[41] R. Krehel, "Research on operation determination of the functional condition of drill bits by means of the resistance method," *Measurement*, vol. 110, pp. 65–73, Nov. 2017.

[42] O. Matthews, R. I. Clayton, and S. Chen, "Drill bit and design method for optimizing distribution of individual cutter forces, torque, work, or power," U.S. Patent 8 437 995 B2, May 7, 2013.

[43] K. R. Goheen and E. R. Jefferys, "The application of alternative modelling techniques to ROV dynamics," in *Proc. IEEE Int. Conf. Robot. Automat.*, Cincinnati, OH, USA, May 1990, pp. 1302–1309.

[44] M. S. W. Bessa, "Controlling the dynamic positioning of a ROV," in *Proc. OCEANS Celebrating Past Teaming Toward Future*, San Diego, CA, USA, 2003, p. 702.

[45] J. Kerdels, J. Albiez, and F. Kirchner, "A robust vision-based hover control for ROV," in *Proc. OCEANS MTS/IEEE Kobe Techno-Ocean*, Kobe, Japan, Apr. 2008, pp. 1–7.

[46] G. E. Guillen and W. G. Lesso, "The use of weight on bit, torque, and temperature to enhance drilling efficiency," in *Proc. Soc. Petroleum Eng. AIME*, vol. spe12165, 1983, pp. 1–12.

[47] T. Feng, H. Zhang, and D. Chen, "Dynamic programming based controllers to suppress stick-slip in a drilling system," in *Proc. Amer. Control Conf. (ACC)*, Seattle, WA, USA, 2017, pp. 1302–1307.

[48] S. P. Barton, H. S. May, and S. Johnson, "Gauge, cutting structure, torque control components—What really counts for optimal tool face control with FC drill bits?" *SPE Drilling, Completion*, vol. 24, no. 2, pp. 293–300, 2009.

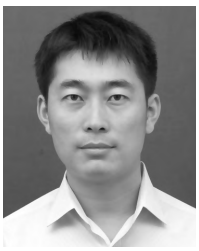

YINGLONG CHEN received the B.Eng. and Ph.D. degrees in mechatronic control engineering from Zhejiang University, Zhejiang, China, in 2008 and 2013, respectively. From 2013 to 2016, he has been a Research Assistant with the School of Mechanical Engineering, Zhejiang University. Since 2017, he has been an Assistant Professor with the Naval Architecture and Ocean Engineering, Dalian Maritime University. His research interests include fluid power transmission and control, advanced motion control of mechatronic systems, and robotics.

HUI LIU received the bachelor's degree in rescue and salvage engineering from Dalian Maritime University, China, in 2018. He is currently pursuing the Ph.D. degree with the Dalian University of Technology. His research interests include mechanical engineering, data mining, and computational fluid dynamics.

ZENGMENG ZHANG received the B.Eng. and Ph.D. degrees in mechatronic control engineering from Zhejiang University, Zhejiang, China, in 2003 and 2009, respectively. Since 2009, he has been a Professor with the Naval Architecture and Ocean Engineering College, Dalian Maritime University. His research interests include fluid power transmission and control, water hydraulics, and artificial muscles.

JIAOYI HOU received the B.Eng. and Ph.D. degrees in mechatronic control engineering from Zhejiang University, Zhejiang, China, in 2007 and 2012, respectively. Since 2012, he has been an Associated Professor with the Naval Architecture and Ocean Engineering College, Dalian Maritime University. His research interests include fluid power transmission and control, and electro-hydraulic proportional control system.

YONGJUN GONG received the Ph.D. degrees in mechatronic control engineering from Zhejiang University, Zhejiang, China, in 2005. Since 2005, he has been a Professor with the Naval Architecture and Ocean Engineering College, Dalian Maritime University. His research interests include fluid power transmission and control, water hydraulics, and underwater tools system.